Detecting wave packet motion in pump–probe experiments: Theoretical analysis

Jianshu Cao and Kent R. Wilson
Department of Chemistry and Biochemistry, University of California, San Diego, La Jolla, California 92093-0339

(Received 5 September 1996; accepted 16 October 1996)

The Zewail–Bersohn model [Ber. Bunsenges. Phys. Chem. **92**, 373 (1988)] of pump–probe experiments is generalized to nonstationary wave packets and more realistic forms of probe pulses. The analysis illustrates the important role of probe linear chirp rate, as pointed out by Sterling, Zadoyan, and Apkarian [J. Chem. Phys. **104**, 6497 (1996)], in detecting the motion of wave packets and the physical reason for the existence of optimal probe pulses to yield the best probe signal. Since the pump–probe process can be viewed as delayed two-photon resonant absorption, the probe signal can be readily optimized within the framework of quantum control theory, as discussed by Yan [J. Chem. Phys. **100**, 1094 (1994)]. Numerical calculations based on quantum control theory are used to confirm our theoretical predictions. We point out that the same analysis can be extended to other impulsive nonlinear optical processes, such as multiphoton pump–probe absorption and stimulated Raman scattering. © *1997 American Institute of Physics.* [S0021-9606(97)01504-3]

I. INTRODUCTION

Femtosecond chemistry offers experimentalists the opportunity to study elementary chemical processes on the molecular level and to directly monitor the dynamical evolution from reactants to products.[1] Femtosecond scale time resolution proves crucial in understanding the basic concepts governing the molecular dynamics of chemical reactions, how they take place, and how to govern them. The key experimental technique in femtochemical spectroscopy is the pump–probe scheme. Many theoretical models have been developed to describe the pump–probe process, including the classical model of Bersohn and Zewail,[2] the classical theory by Walkup *et al.*,[3] the generalized linear response theory by Lin and co-workers,[4] the analysis by Pollard *et al.*,[5] the extensive work on nonlinear spectroscopy by Yan and Mukamel,[6,7] and others. A review on this subject can be found in Lee[8] and the references cited therein. In this paper, we will present a theoretical analysis of pump–probe spectroscopy, in particular the probe process, within the classical and semiclassical framework, along with a treatment from the point of view of optimal quantum control theory.[9–11]

Using transient probe absorption to detect wave packets has been discussed in different contexts, including the optimal control of molecular dynamics.[12] More recently, Sterling, Zadoyan, and Apkarian[13] investigated the effect of linear chirped pulses in condensed phase pump–probe experiments by classical simulations for the model system of I_2 isolated in a Kr matrix, and predicted that chirped probe pulses can be employed to characterize the momentum of an evolving molecular wave packet. They transformed the frequency-time profile of the probe pulse to coordinate-time space and noted that the observable signal is a function of the relative group velocities of the traveling wave packet and the traveling window function. In fact, the prediction agrees qualitatively with preliminary experiments on I_2 and NaI in our lab. In our paper, we analyze the pump–probe process in a systematic and rigorous fashion and justify this effect within the semiclassical framework.

A one-dimensional wave packet picture of pump–probe spectroscopy is shown schematically in Fig. 1, where the three electronic states involved in the process are sketched: the ground, the first excited (pump), and the second excited state (probe). Assuming the molecule is initially in the ground state, the pump pulse promotes the wave function onto an excited state, where the excited state wave packet propagates with time. Then, the probe pulse, after a certain delay time with respect to the pump pulse, promotes the evolving wave packet to the second excited state, where the wave packet either dissociates to products or decays to lower-lying states. Three types of experimental results[14–16] are thus accessible: (1) detection of the fragments and (2) laser-induced fluorescence (LIF), which are both integrated pump–probe signals (IPP), as a function of the probe carrier frequency and the delay time. The third type of the measurement is (3) the dynamic dispersed absorption spectra of the probe pulse after passing through the sample, also termed the dispersed pump–probe signal (DPP), as a function of the delay time. In this paper we will deal only with the first (IPP) kind of signal.

Femtosecond pump–probe spectroscopy, viewed as a nonlinear two-photon process, is described[6] by the third-order polarization $P^{(3)}$, a function of the pump–probe delay time. In Sec. II, it is shown that when the pump and probe pulses are well separated, the pump–probe process is a two-step sequential excitation consisting of one stationary absorption and one nonstationary absorption. Of conceptual importance is the introduction of the initial wave function which is the net result of a laser excitation without any further spreading. In Appendix A, the IPP signals are expressed in terms of their initial wave function induced by the probe pulse.

The primary feature of femtospectroscopy is the extremely short time duration of laser pulses such that the

 0021-9606/97/106(12)/5062/11/$10.00

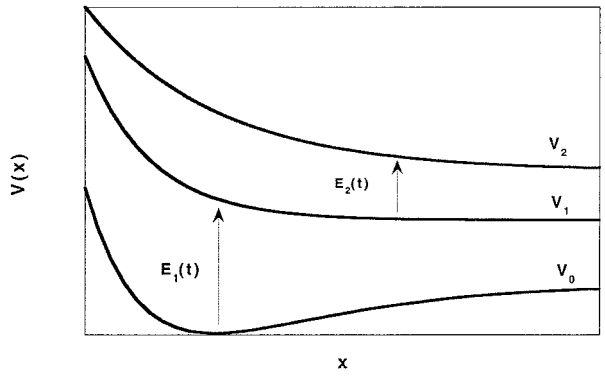

FIG. 1. An illustration of pump–probe processes. Assuming the molecule is initially in the ground state, $|0\rangle$, the pump pulse, E_1, promotes the wave function onto an excited state $|1\rangle$, where the excited state wave packet propagates with time. Then, the probe pulse, E_2, after a certain delay time with respect to the pump pulse, promotes the evolving wave packet to a second excited state, $|2\rangle$, where the wave packet either dissociates to products or decays to lower-lying states.

nuclear wave packet can often be assumed frozen during excitation.[17–20] Under this assumption, the excited state or probe state wave function can be obtained in a closed form and thus effects of the optical pulse can easily be investigated. As an example, the analytical nature of this approximation has been recently used in studying the relationship between the linear chirp rate of the pump field and the vibrational localization of the wave packet motion induced by the pump pulse.[21] In Sec. III and Appendix B, the validity and implications of the frozen wave packet assumption are carefully analyzed. The application of this approximation to the probe process leads to the Bersohn–Zewail classical model[2] discussed in Sec. III. It is suggested within this model that, in order to abstract information about the pump wave packet from the signal, the probe pulse should be short enough that the motion of the wave packet does not smear the signal and at same time be long enough to have sufficient spectral resolution.

In Sec. IV, we relax the frozen wave packet assumption to incorporate the constant motion of the molecular wave packet and thus generalize the Bersohn–Zewail classical model to a more realistic theory. To do this, the kinetic energy operator is applied twice to a Gaussian wave packet as described in Appendix C, the formula for IPP signals is evaluated for a Gaussian laser pulse, and consequently an explicit expression for the spatial resolution of the probe pulse is obtained. As a result of this nonstationary semiclassical analysis, an optimal pulse duration for transform limited laser pulses is derived and a linear relation between the chirp of the optimal probe pulse and the motion of the pump wave packet is predicted.[13] The classical analysis in Sec. III and the semiclassical analysis in Sec. IV can be extended to other multiphoton processes, such as off-resonant two-photon absorption, studied in Appendix D.

Theory[22–26] has been developed to predict an optimal laser field to drive a quantum wave packet to a desired functional form at a chosen time. However, most efforts have been made toward single field quantum control, mainly the pump process. For example, the I_2 experiment reported by Kohler *et al.*[27,28] is designed to focus the molecular wave packet to a designated minimum uncertainty wave packet for the pump state wave function,[10] with the probe process treated as a detection device.[12] To generalize the single field theory, we formulate optimal control theory for an arbitrary sequential multiphoton process in Appendix E and to pump–probe processes in Sec. V, extending previous work by Rice,[29] Tannor,[9] and Yan.[11] More pertinent to this paper, we restrict the optimization procedure to the probe process for a given pump state wave function in Sec. V where optimization of the pump–probe signal is used to maximize the spatial resolution of the probe pulse. Numerical examples of the optimization of the probe process based on an idealized model confirm the linear relation between the optimal linear chirp rate and the constant velocity of the wave packet.[13]

In summary, the probe process in pump–probe experiments is studied in the framework of the Bersohn–Zewail classical model, semiclassical nonstationary analysis, and optimal control theory. The validity of the assumptions and approximations used are rigorously established and numerical examples are presented to verify the theoretical prediction. Finally, a discussion in Sec. VI concludes the paper.

II. WAVE PACKET MODEL OF THE SEQUENTIAL PUMP–PROBE PROCESS

The molecular system consists of three electronic states, $|0\rangle$, $|1\rangle$, and $|2\rangle$, described by three diabatic Hamiltonians, $\hat{H}_0$ for the ground state $|0\rangle$, $\hat{H}_1+\hbar\omega_{10}$ for the intermediate excited (pump) state $|1\rangle$, and $\hat{H}_2+\hbar\omega_{21}+\hbar\omega_{10}$ for the final excited (probe) state $|2\rangle$. Here, $\omega_{10}=\omega_1-\omega_0$ and $\omega_{21}=\omega_2-\omega_1$ are the electronic transition frequencies between the corresponding states. This three-level molecule then couples via a dipole interaction to time-dependent electric fields which are treated classically as

$$\epsilon_1(t)=E_1(t)e^{-i\omega_{10}t}+E_1^*(t)e^{i\omega_{10}t} \tag{1}$$

for the pump pulse, and

$$\epsilon_2(t)=E_1(t)e^{-i\omega_{21}t}+E_1^*(t)e^{i\omega_{21}t} \tag{2}$$

for the probe pulse. Within the rotating wave approximation, the total Hamiltonian is expressed as

$$\hat{H}(t)=\hat{H}_M+\hat{H}_{pu}+\hat{H}_{pr}, \tag{3}$$

where the molecular term is the three-level Hamiltonian

$$\hat{H}_M=\hat{H}_0|0\rangle\langle 0|+\hat{H}_1|1\rangle\langle 1|+\hat{H}_2|2\rangle\langle 2|, \tag{4}$$

the interaction term for the pump pulse is

$$\hat{H}_{pu}(t)=-\mu_1E_1^*(t)|0\rangle\langle 1|-\mu_1E_1(t)|1\rangle\langle 0|, \tag{5}$$

with μ_1 being the transition dipole moment between states $|0\rangle$ and $|1\rangle$, the interaction term for the probe pulse is

$$\hat{H}_{pr}(t)=-\mu_2E_2^*(t)|1\rangle\langle 2|-\mu_2E_2(t)|2\rangle\langle 1|, \tag{6}$$

with μ_2 being the transition dipole moment between states $|1\rangle$ and $|2\rangle$, and the dipole transition between states $|0\rangle$ and $|2\rangle$ is assumed to be prohibited.

Since there are two laser fields which play a role, the leading term in the final probe state wave function is given to second order in the dipole interaction by

$$\psi(t_f)=\left(\frac{i}{\hbar}\right)^2\int_{t_i}^{t_f}dt_2\int_{t_i}^{t_2}dt_1 e^{-i\hat{H}_M(t_f-t_2)/\hbar}(\hat{H}_{pu}+\hat{H}_{pr}) \times e^{-i\hat{H}_M(t_2-t_1)/\hbar}(\hat{H}_{pu}+\hat{H}_{pr})e^{-i\hat{H}_M(t_1-t_i)/\hbar}\psi(t_i), \quad (7)$$

where $\psi(t_f)$ and $\psi(t_i)$ are the wave functions at the final time t_f and the initial time t_i, respectively. To be more specific to the pump–probe scenario, the molecule, initially in its ground state $\psi(t_i)=\psi_0|0\rangle$, is excited by the pump field $E_1(t)$ to excited state $|1\rangle$, and then by the probe field $E_2(t)$ to excited state $|2\rangle$. It is assumed that the pump and probe pulses do not overlap in time and that the centers of the two pulses are separated by a delay time τ. In other words, the pump pulse is centered at $t=0$, the probe pulse is centered at $t=\tau$, and the time durations of the two pulses are assumed to be substantially smaller than the delay time τ. Taking these factors into consideration, the probe state wave function in Eq. (7) can be simplified as

$$\psi_2(t_f)=\left(\frac{i}{\hbar}\right)^2\int_{t_i-\tau}^{t_f-\tau}dt_2'\int_{t_i}^{t_2'+\tau}dt_1 e^{-i\hat{H}_2(t_f-t_2'-\tau)/\hbar} \times\mu_2 E_2^{\tau}(t_2')e^{-i\hat{H}_1(t_2'+\tau-t_1)/\hbar}\mu_1 E_1(t_1)e^{-i\hat{H}_0(t_1)/\hbar}\psi_0, \quad (8)$$

where the time variable t_2 is shifted according to $t_2' = t_2 - \tau$ and the probe field is redefined as $E_2^{\tau}(t_2') = E_2(t_2' + \tau)$. Furthermore, because the two pulses are well-separated in time and the detection time t_f is much larger than the terminal time of the probe pulse, we are allowed to extend the integral limits of t_1 and t_2' to infinity. The resulting expression can be cast in a revealing format,

$$\psi_2(t_f)=e^{-i\hat{H}_2(t_f-\tau)/\hbar}\psi_2(\tau), \quad (9)$$

$$\psi_2(\tau)=\frac{i}{\hbar}\int_{-\infty}^{\infty}e^{i\hat{H}_2 t}\mu_2 e^{-i\hat{H}_1 t}\psi_1(\tau)E_2(t)dt, \quad (10)$$

$$\psi_1(\tau)=e^{-i\hat{H}_1\tau}\psi_1, \quad (11)$$

$$\psi_1=\frac{i}{\hbar}\int_{-\infty}^{\infty}e^{i\hat{H}_1 t}\mu_1 e^{-i\hat{H}_0 t}\psi_0 E_1(t)dt, \quad (12)$$

where, for the simplicity of notation, the superscript τ in E_2^{τ} is dropped, and both t_2' and t_1 are replaced with t.

By writing Eqs. (9)–(12), the pump–probe process is treated as a sequential two-photon process described by a wave packet picture[30,31] with ψ_1 representing the initial pump wave packet on $|1\rangle$ created by the pump pulse $E_1(t)$, $\psi_1(\tau)$ the propagating wave packet on $|1\rangle$ at the delay time τ, $\psi_2(\tau)$ the initial probe wave packet on $|2\rangle$ created by the probe pulse $E_2(t)$, and $\psi_2(t_f)$ the final probe wave packet on $|2\rangle$ at the detection time t_f. The concept of the initial wave function,[21] ψ_1 and $\psi_2(\tau)$, refers to the immediate result of a laser pulse, excluding any further vibrational propagation on the excited state potential surface, and thus contains all the necessary information about the electronic excitation.

It is shown in Appendix A that all the integrated signals are related to the population on the probe state,

$$N(\tau)=\langle\psi_2(t_f)|\psi_2(t_f)\rangle=\langle\psi_2(\tau)|\psi_2(\tau)\rangle, \quad (13)$$

where the detection time t_f is set after the probe pulse has terminated and Eq. (9) is used to help obtain the second equality. Therefore, the initial wave function on the probe state potential surface as a function of the delay time τ fully determines the time evolution of the integrated pump–probe signals.

A careful examination of the initial pump wave function $\psi_2(\tau)$ and the initial probe wave function ψ_1 reveals the essential difference between the pump and probe processes: ψ_0 in Eq. (12) is stationary under the operation of $\hat{H}_0$ (an eigenstate of $\hat{H}_0$) whereas $\psi_1(\tau)$ in Eq. (10) is nonstationary under the operation of $\hat{H}_1$. In this sense, the probe process can be viewed from the point of nonstationary absorption spectroscopy in contrast to the stationary excitation from the ground state induced by the pump pulse. Since the pump and probe processes can be treated separately and the impulsive excitation from the ground state has been well studied within the classical and semiclassical approximations, the focus of this paper is to investigate the probe process given an excited state wave packet moving on the pump state potential surface, that is, the evaluation of $\psi_2(\tau)$ for a given pump state wave function $\psi_1(\tau)$.

III. BERSOHN–ZEWAIL CLASSICAL MODEL: THE STATIONARY ASSUMPTION

The duration of the probe laser pulse used to detect the wave packet is usually sufficiently small that the nuclear configuration is approximately frozen during the probe excitation. This observation constitutes the core assumption underlying the well-known Bersohn–Zewail classical model,[2] which amounts to a coordinate-dependent two-level-system approximation by ignoring the kinetic energy operator.[17–20] The stationary assumption is valid only if δx, the displacement of the center of the wave packet during excitation, is substantially smaller than λ, the width of the wave packet at the time of excitation, that is

$$\delta x(t_p)\ll\lambda, \quad (14)$$

where δx is a function of t_p, the time duration of the probe pulse. Since the wave function on the pump state potential surface is a moving wave packet, the displacement consists of two parts: the contribution from the initial velocity v_c before the excitation, given by

$$t_p v_c\ll\lambda, \quad (15)$$

and the contribution from the acceleration during the excitation, given by

$$\frac{f_c}{m}t_p^2\ll\lambda, \quad (16)$$

where f_c is the force due to the potential difference in the Franck–Condon region. The condition in Eq. (15) is self-evident whereas the condition in Eq. (16) is confirmed in Appendix B by making use of the displaced harmonic oscillator model. Both conditions are satisfied if the motion of the wave packet is slow and the coordinate dependence of the potential difference is weak.

Under the frozen wave packet assumption, the kinetic energy operator is ignored in Eq. (10), resulting in the initial probe state wave function as

$$\psi_2(\tau)=\frac{i}{\hbar}\int_{-\infty}^{\infty}e^{i\omega(x)t}\mu_2 E_2(t)dt\psi_1(\tau), \tag{17}$$

where the coordinate-dependent frequency $\hbar\omega(x)$, or $U(x)$, is the potential difference between excited states $|1\rangle$ and $|2\rangle$,

$$U(x)=\hbar\omega(x)=V_2(x)-V_1(x). \tag{18}$$

With the Fourier transformation of the electric field defined as

$$\tilde{E}(\omega)=\int_{-\infty}^{\infty}E(t)e^{i\omega t}dt, \tag{19}$$

the expression for the integrated pump–probe signal, Eq. (13), becomes

$$N(\tau)=\frac{1}{\hbar^2}\langle\psi_1(\tau)|[\mu_2(x)]^2|\tilde{E}_2[\omega(x)]|^2|\psi_1(\tau)\rangle, \tag{20}$$

which represents the central result of the Bersohn–Zewail classical model.[1,2,8]

For illustration, we take the example of a chirped Gaussian pulse defined as

$$E_G(t)=E_0\ \exp\left[-\frac{(t-t_0)^2}{2t_p^2}-i\omega_0(t-t_0)-ic\ \frac{(t-t_0)^2}{2}\right], \tag{21}$$

where five parameters are employed to characterize the light pulse: an amplitude E_0, a carrier frequency ω_0, a temporal center t_0, a temporal width t_p, and a linear chirp rate c, respectively. From Eq. (19), the corresponding power spectrum reads

$$P(\omega)=|\tilde{E}_G(\omega)|^2=P_0\ \exp\left[-\frac{(\omega-\omega_0)^2}{\Gamma^2}\right], \tag{22}$$

where the magnitude is $P_0=2\pi t_p E_0^2/\Gamma$ and the bandwidth is defined as

$$\Gamma^2=c^2t_p^2+\frac{1}{t_p^2}, \tag{23}$$

which is related to the full width half maximum of the power spectrum by $\Delta\omega_{\mathrm{FWHM}}=2\sqrt{\ln 2}\Gamma$.

It can be seen from Eqs. (20) and (22) that the probe pulse opens a window on the pump state potential surface and transfers the population within the window into the pump–probe signal. To determine the size of this window, namely the spatial resolution, we expand the coordinate-dependent frequency $\omega(x)$ to linear order in x, giving

$$\omega(x)=\omega_0+g(x-x_0)+\cdots, \tag{24}$$

where ω_0 is the carrier frequency of the probe pulse, x_0 is the Franck–Condon point corresponding to the carrier frequency, i.e., $w_0=w(x_0)$, and g is the linear coefficient of the Taylor expansion of $\omega(x)$ at x_0. For a transform limited Gaussian pulse, i.e., $c=0$, Eq. (20) becomes

$$N(\tau)=\frac{P_0}{\hbar^2}\langle\psi_2(gt)|[gm_2(x)]^2 \times\exp[-g^2t_p^2(x-x_0)^2]|\psi_2(\tau)\rangle, \tag{25}$$

which defines the spatial resolution as

$$\alpha=\frac{1}{gt_p}. \tag{26}$$

In order to abstract valuable information about the spatial distribution of the wave packet from the pump–probe signal, the spatial resolution of the signal must be smaller than the characteristic width of the molecular wave packet, that is,

$$\alpha\ll\lambda, \tag{27}$$

or

$$t_p\gg\frac{1}{g\lambda}, \tag{28}$$

implying that a pulse of long time duration is preferred. On the other hand, Eqs. (15) and (16) require the pulse to be short enough that the displacement of the wave packet during the excitation is substantially smaller than the width of the wave packet. Consequently, there exists an optimal pulse duration which gives the best compromise between these two opposing factors. In next section, this optimal pulse duration will be determined by a rigorous analysis.

The above formulation parallels the analysis of the pump process in the classical approximation,[21] since the moving wave packet is treated as frozen just as in the case of the excitation from the ground state. To reflect the special features of the probe process, one must take into account the crucial difference that the wave function on the excited state potential surface is in motion whereas the wave function on the ground state potential surface is at rest. This consideration leads to the nonstationary analysis of the next section.

IV. GENERALIZED BERSOHN–ZEWAIL MODEL: NONSTATIONARY ANALYSIS

To investigate the effects of the initial motion of the delayed pump wave packet on the probe signal, we will lift the stationary assumption imposed by the frozen wave packet approximation. To begin, the quantum propagator is split into the kinetic energy and potential energy parts by making use of an operator identity

$$e^{i\hat{H}t}=e^{i(\hat{K}+\hat{V})t}=e^{i\hat{K}t/2}\ \exp[i\hat{V}t+O(t^3)]e^{i\hat{K}t/2}, \tag{29}$$

which is accurate to the third order in time. Then, the initial

probe state wave function in Eq. (10) can be rewritten as

$$\psi_2(\tau)\approx\frac{i}{\hbar}\int_{-\infty}^{\infty}e^{i\hat{K}t/2}e^{i\hat{U}t}e^{-i\hat{K}t/2}E_2(t)dt\psi_1(\tau), \tag{30}$$

where $\hat{U}=\hat{V}_2-\hat{V}_1$ is the potential difference, the transition dipole moment is taken as a constant, $\mu=1$, and $\hbar$ is omitted for simplicity of presentation. If the potential energy operator $\hat{U}$ and the kinetic energy operator $\hat{K}$ are allowed to commute, the two free particle operators $e^{i\hat{K}t}$ and $e^{-i\hat{K}t}$ in Eq. (30) cancel each other and the classical result in Eq. (17) is recovered. Therefore, Eq. (30) represents a more accurate and general description of impulsive excitation and detection processes than the classical treatment discussed above.

In the probe process, the constant velocity motion of the wave packet is usually the dominant factor in comparison to the net acceleration, implying that Eq. (15) is a more stringent constraint on the pulse duration than Eq. (16). Since Eq. (30) takes into account the constant motion of the wave packet, the constrain of Eq. (15) can be removed while the condition in Eq. (16) remains imposed. To satisfy Eq. (16), assumptions are made in writing Eq. (30) that (i) the probe pulse is relatively short and (ii) the wave packet is located in a relatively flat region on both the pump and probe state potential surfaces such that the centroid velocity of the wave packet remains constant during excitation.

In Eq. (30), the first free particle operator $e^{-i\hat{K}t/2}$ propagates the delayed wave function $\psi_1(\tau)$ forward for time $t/2$, whereas the second free particle operator $e^{i\hat{K}t/2}$ propagates backward for time $t/2$ along with the phase factor $e^{i\hat{U}t}$. Therefore, if it were not for the phase factor, the two kinetic energy propagators would cancel, giving rise to the classical approximation. To perform these operations explicitly, let us consider the simple case of a Gaussian wave packet defined as

$$\psi_1(\tau)=\frac{1}{(\pi\lambda^2)^{1/4}}\exp\left[-\frac{(x-x_c)^2}{2\lambda^2}+i\,\frac{p_c(x-x_c)}{\hbar}\right], \tag{31}$$

where x_c, v_c, and p_c are the position, velocity, and momentum of the center of the molecular wave packet in phase space, respectively. Here, the position, velocity, and momentum are measured at the delay time τ and are thus functions of τ implicitly. It is shown in Appendix C that, under the condition of $\hbar t/m\ll\lambda^2$, the free particle propagation of a Gaussian wave packet retains the Gaussian functional form and can be expressed by classical dynamical quantities. In addition, we adopt the linear expansion of the potential difference as in Eq. (24). After substituting Eqs. (24) and (30) into Eq. (31) and applying the free particle propagation in Eq. (C7) twice, we have

$$\psi_2(\tau)=\frac{i}{\hbar}\int_{-\infty}^{\infty}e^{i\omega_0 t}E_2(t)\Psi(\tau,t)dt, \tag{32}$$

where

$$\begin{aligned}\Psi(\tau,t)&=e^{i\hat{K}t/2}e^{igxt}e^{-i\hat{K}t/2}\psi_1(\tau)\\&=\frac{1}{(\pi\lambda^2)^{1/4}}\exp\left[-\frac{(x-x_c)^2}{2\lambda^2}+ip_c(x-x_c)\right.\\&\quad\left.+igxt+i\,\frac{v_c g t^2}{2}\right].\end{aligned} \tag{33}$$

The last term in Eq. (33) reflects the coupling between the nuclear motion and the potential difference $\hat{U}$. Consequently, the expression for the signal, Eq. (13), can be expressed as

$$\begin{aligned}N(\tau)=&\int dt\int dt'\int dx e^{i\omega_0(t-t')}E(t)E^*(t')\\&\times\Psi(\tau,t)\Psi^*(\tau,t'),\end{aligned} \tag{34}$$

which, after the integration over the spatial coordinate, becomes

$$\begin{aligned}N(\tau)=&\int dt\int dt' E(t)E^*(t')\exp\{-(\lambda gs)^2\\&+igs(2x_c+v_c t+v_c t'-2x_0)\},\end{aligned} \tag{35}$$

with $2s=t-t'$ and $\hbar\omega_0=U(x_0)$. Here, both x_c and v_c are implicit functions of the delay time τ. To be consistent with the analytical nature of this analysis, various functional forms of the probe field, such as a Lorentzian spectral intensity, an exponential-decay field, and a Gaussian pulse, can be used for the evaluation of Eq. (35).

For illustration, the Gaussian form of the light pulse defined in Eq. (21) is substituted into Eq. (35) and the double time integrals are completed, resulting in

$$N(\tau)\propto\frac{1}{\Lambda}\exp\left[-\frac{1}{\Lambda^2}(x_c-x_0)^2\right], \tag{36}$$

where Λ measures the spatial dependence of the probe signal, given by

$$\Lambda^2=\lambda^2+\frac{1}{g^2t_p^2}+t_p^2\left(v_c-\frac{c}{g}\right)^2. \tag{37}$$

Λ^2 characterizes the decay of the probe signal as the center of the wave packet moves out of the probe window, or equivalently, the sensitivity of the probe signal with respect to the change in its carrier frequency.

By comparison with the functional form of the Gaussian wave packet in Eq. (21), the first term in Eq. (37) is recognized as the width of the wave packet being detected and the rest of the terms in Eq. (37) define the spatial resolution of the signal,

$$\alpha^2=\frac{1}{g^2t_p^2}+t_p^2(v_c-c/g)^2, \tag{38}$$

which, as stated earlier, determines the size of the probe window. The smaller α is, the more accurate is the one-to-one correspondence between the carrier frequency of the probe pulse and the centroid position of the wave packet being probed, and consequently the more prominent are the peaks of the probe signal. Therefore, the optimization of the

pump–probe signal is equivalent to the minimization of the spatial resolution, α. We now explicitly consider transform-limited and chirped laser pulses.

(1) For a transform-limited laser pulse, $c=0$, the spatial resolution in Eq. (38) becomes

$$\alpha^2=\frac{1}{t_p^2 g^2}+t_p^2 v_c^2. \tag{39}$$

By minimizing α, we find an optimal pulse duration

$$t_p^2=\frac{1}{g v_c}, \tag{40}$$

which has been argued in the previous section within the classical model.

(2) As seen from Eq. (38), the primary condition for minimizing the spatial resolution of a chirped probe pulse is

$$c=v_c g, \tag{41}$$

meaning that the shift of the carrier frequency with time shall follow the motion of the wave packet as predicted by Sterling *et al.*[13] With the chirp rate given as above, the spatial resolution becomes

$$\alpha=\frac{1}{t_p g}\ll\lambda, \tag{42}$$

which is minimized by increasing the pulse duration. On the other hand, the constraint in Eq. (16) still applies, which together with Eq. (42) again leads to an optimal value of pulse duration.

Hence, the nonstationary semiclassical analysis not only confirms the argument of the classical model quantitatively, but also provides new insights unavailable in the strictly classical framework. The semiclassical analysis presented in this section and the classical analysis discussed in last section can also be applied to a wide range of nonlinear impulsive processes, such as multiphoton pump–probe absorption and stimulated Raman scattering. In Appendix D, we analyze off-resonant two-photon absorption with the help of the classical model and find that under the frozen wave packet assumption the two-photon process can be approximately treated as a single photon process with an effective excitation laser pulse with double the carrier frequency, double the linear chirp rate, and the square of the field amplitude.

To verify the analysis in this section, a numerical procedure is required to optimize the probe resolution under certain constraints, that is, the optimization of the probe process. Therefore, the optimization formulation in next section and in Appendix E serves not only the goal of the optimal quantum control of matter wave packets by tailored laser pulses but also as a means to test our theory for detecting wave packet motion in pump–probe experiments.

V. OPTIMIZATION OF PUMP–PROBE SIGNALS

As described in Sec. III, the general optimization procedure for a sequential multiphoton process can be formulated with the help of optimal quantum control theory. We now focus on the pump–probe process, a sequential two-photon excitation. As pointed out earlier, the physical quantity of interest is the population on the probe state, $N(\tau)$ in Eq. (13), which defines the target operator to be the identity operator $\hat{A}=\hat{I}_2$ defined on the probe state potential surface. The molecule is assumed to be initially in a pure state $\rho_0=|\psi_0\rangle\langle\psi_0|$ on the ground electronic state manifold. Applying Eq. (E 11) in Appendix E to the pump–probe process as described above, we have the optimization equation for the probe field,

$$\int_{t_0}^{t_i} dt_2'\langle\psi_1(t_2)|G_2^+(t_f-t_2)G_2(t_f-t_2)|\psi_1(t_2')\rangle E_2(t_2') = \eta_2 E_2(t_2), \tag{43}$$

where the pump state wave function $\psi_1(t_2)$ is

$$\psi_1(t_2)=G_1(t_2-t_1):G_0(t_1-t_i)\psi_0, \tag{44}$$

and the optimization equation for the pump field,

$$\int_{t_i}^{t_f} dt_1\langle G_0(t_1-t_i)\psi_0|A_1(t_1,t_1')|G_0(t_1'-t_i)\psi_0\rangle E_1(t_1') = \eta_1 E_1(t_1), \tag{45}$$

where the target for the pump field is

$$A_1(t_1,t_1')=G_1^+(t_2-t_1):G_2^+(t_f-t_2)G_2(t_f-t_2):G_1(t_2-t_1). \tag{46}$$

The colon in the above equation represents an electric excitation as defined in Eq. (E4). Notice that the eigenequation for the probe field $E_1(t)$ depends implicitly on the pump field $E_2(t)$, and vice versa. Hence, Eqs. (43) and (45) are solved independently for a given input; the resulting optimal fields are then used as the input for the next iteration, and this procedure is repeated until convergence is reached. Similar optimization procedures have been proposed before by Yan.[11]

To be relevant to the theme of this paper, we will further limit the optimization to the probe process. To this end, we make use of the concept of the initial wave function introduced in Sec. II and rewrite Eq. (43) as

$$\int_{t_i}^{t_f} M(t,t')E_2(t')dt'=\eta_2 E_2(t), \tag{47}$$

where the material response matrix reads

$$M(t,t')=\langle\psi_1(\tau)G_1(t)G_2(t_f-t)|G_2(t_f-t') \times G_1(t')\psi_1(\tau)\rangle, \tag{48}$$

with the initial wave function on the excited state at the delay time τ, $\psi(\tau)$, defined by Eq. (12). As argued in Sec. IV, for a given wave packet moving on the pump state surface, the optimization of the pump–probe signal is equivalent to the optimization of the probe resolution. In particular, we will investigate the relation between the linear chirp rate of the optimal probe pulse and the centroid velocity of the molecular wave packet.[13]

To simplify the analysis, the pump state potential is taken as a constant, $V_1=0$, the probe state potential is taken as a linear harmonic oscillator, $V_2=m\omega^2 x/2$. The probe state wave function then takes the Gaussian form,

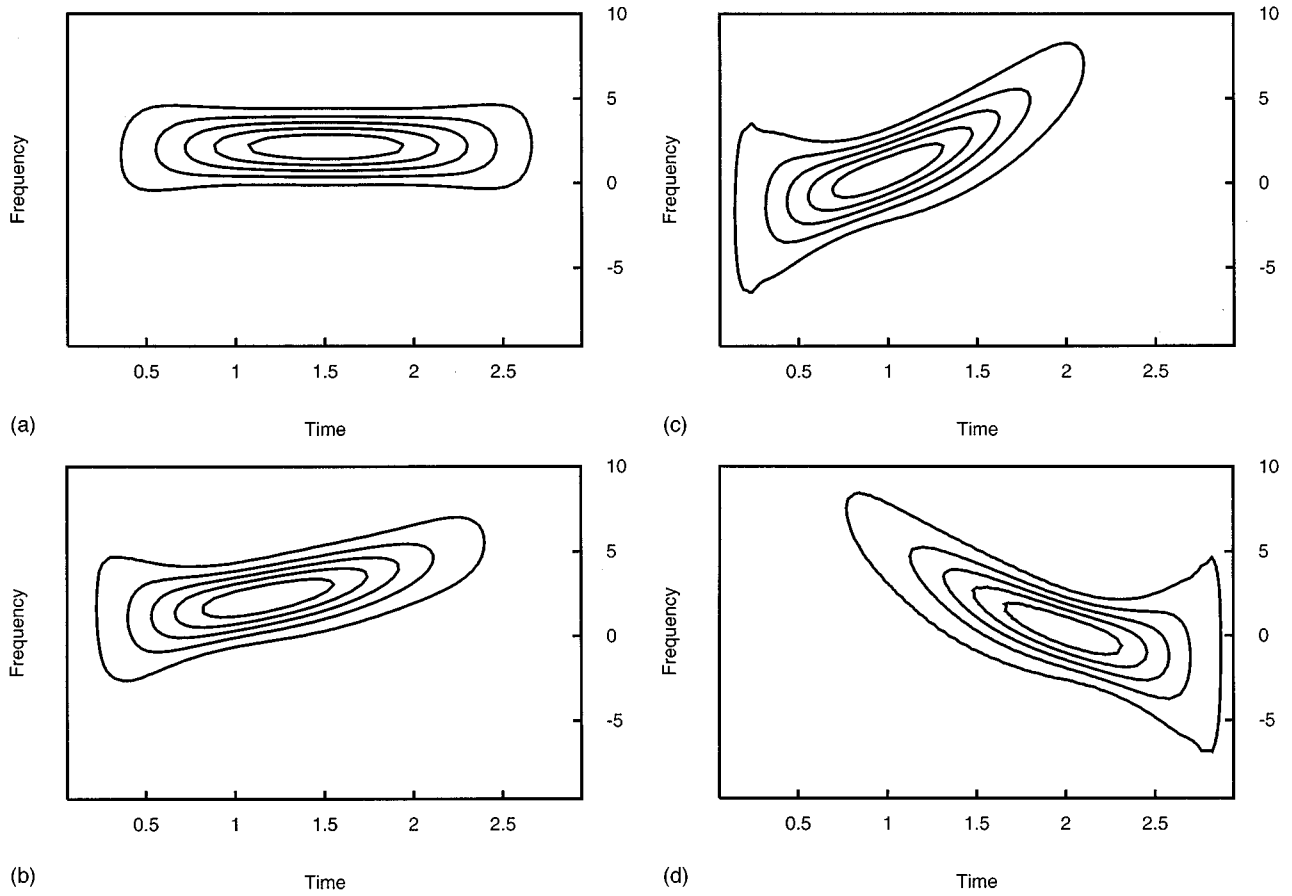

FIG. 2. Contours plots of the Wigner transformation of the optimal probe fields for the wave packet of $x_c=2$ and $v_c=0$ in (a), for $x_c=1$ and $v_c=1$ in (b), for $x_c=0$ and $v_c=2$ in (c), and for $x_c=6$ and $v_c=-2$ in (d), respectively.

$$\psi_1(t)=\frac{1}{(\pi\lambda^2)^{1/4}}\exp\left[-\frac{(x-x_c-v_ct)^2}{2\lambda^2}+i\,\frac{p_c(x-x_c-v_ct/2)}{\hbar}\right], \tag{49}$$

which is shown to satisfy the Schrödinger equation in Appendix C. Here, all nonessential parameters, m, ω, λ, and $\hbar$, assume the unit value. The initial position of the wave packet x_c has been adjusted according to its initial velocity v_c so that the probe window is approximately set at $x_0=2$ corresponding to a carrier frequency of $\omega_0=2$. The probe state propagator G_2 in Eq. (48) can be obtained in a closed from for the harmonic oscillator potential and the coordinate integration of the response function in Eq. (48) can be performed analytically. The time range for the probe pulse is $t_i=0$ and $t_f=3$, and the response matrix is evaluated on a time grid of $dt=0.03$. Then the discretized material response matrix is diagonalized and the optimal electric field thus obtained.

The Fourier transformation of the Gaussian pulse of Eq. (21) can be expressed as

$$E_G(\omega)=E_0\sqrt{\frac{\pi t_p^2}{1+ict_p^2}}\exp\left[i\omega t_0-\frac{(\omega-w_0)^2}{2\Gamma^2}-ic'\,\frac{(\omega-w_0)^2}{2}\right], \tag{50}$$

where c' is the linear chirp rate in the frequency domain, which is related the linear chirp rate in the time domain by[21]

$$c'=\frac{ct_p^2}{\Gamma^2}. \tag{51}$$

The chirp of a laser pulse describes the correlation between frequency and time, which cannot be deduced from the temporal envelope or the power spectrum. The electric field can be represented in the Wigner transformation form,[10]

$$F(t,\omega)=\int_{-\infty}^{\infty}d\tau e^{-i\omega\tau}E^*(t+\tau/2)E(t-\tau/2), \tag{52}$$

which reduces to the power spectrum $|E(\omega)|^2$ when integrated over the time variable and reduces to the temporal field strength $|E(t)|^2$ when integrated over the frequency variable. Substituting the Gaussian field Eq. (21) into Eq. (52), we have

$$F_G(t,\omega)=E_0^2\ \exp\left\{-\frac{(t-t_0)^2}{t_p^2}-t_p^2[(\omega-\omega_0)-c(t-t_0)]^2\right\}, \tag{53}$$

which clearly shows that the center of the frequency $\omega_0+c(t-t_0)$ shifts at the rate of the linear chirp c. Generally speaking, on the $F(t,\omega)$ contour diagram, there is a center frequency at each time, these centers form a principal axis of the contour plot as a function of time, and the slope defined as the tangent formed by this principal axis and the time axis is equal to the time domain linear chirp rate.

The contours of the Wigner transform of the optimal fields are shown for various molecular wave packets, $x_c=2$ and $v_c=0$ in Fig. 2(a), $x_c=1$ and $v_c=1$ in Fig. 2(b), $x_c=0$ and $v_c=2$ in Fig. 2(c), and $x_c=6$ and $v_c=-2$ in Fig. 2(d). As can be seen from the slopes of the contours in these figures, the optimal probe pulse for a stationary wave packet is a transform limited pulse, the optimal probe pulse for a molecular wave packet moving to the right has a positive linear chirp rate, and the optimal probe pulse for a molecular wave packet moving to the left has a negative linear chirp rate, as expected from our analysis. In fact, the linear chirp rates are $c=0$ in Fig. 2(a), $c=2$ in Fig. 2(b), $c=4$ in Fig. 2(c), and $c=-4$ in Fig. 2(d), which agree exactly with the prediction in Eq. (41).

VI. CONCLUSION

The Bersohn–Zewail classical model in Sec. III is generalized to a nonstationary analysis in Sec. IV, and this is used to theoretically verify the correlation between the chirp of the optimal probe pulse and the motion of the molecular wave packet being probed, as discussed by Sterling, Zadoyan, and Apkarian.[13] With Eq. (41), information can be learned from a generalization of pump–probe experiments, with the coordinate of the molecule being measured by the carrier frequency and the velocity corresponding to the molecular coordinate measured by the linear chirp rate of the optimal laser pulse. Consequently, by tailoring the probe laser pulse to yield the highest signal peak, the trajectory of the molecular wave packet can be mapped out in phase space. Such experimental techniques may be useful in studying molecular dynamics during chemical reactions as well as vibrational relaxation and dephasing in condensed phases.

To test the validity of our semiclassical prediction of the optimal probe pulse, we apply quantum optimal control theory and find excellent agreement. The general multiphoton quantum control formulation given in Appendix E is not limited to a single photon process. For example, the two-pulse formulation for the pump–probe process can be used to maximize the yield of product at a target time in the context of quantum control. It will be interesting to compare the result obtained from the two-pulse optimization and the result from a single-pulse optimization.

ACKNOWLEDGMENT

We thank Dr. Chris Bardeen for his help with respect to the latest experimental developments on this subject.

APPENDIX A: INTEGRATED PUMP–PROBE SIGNALS

The derivation and definitions in this appendix follow closely the review paper[8] by Lee on this subject. In pump–probe experiments, the fluorescence signal or the yield of photofragments from the second excited (probe) state are measured as a function of the pump–probe delay time, τ. Theoretically, all integrated pump–probe (IPP) signals can be described by two kinds of quantities: the total energy loss per unit area by the probe pulse, also known as the integrated pump–probe energy (IPPe) signal, defined by

$$I(\tau)=\frac{1}{2\pi}\int_{-\infty}^{\infty}I_{pr}(\omega,\tau)d\omega, \tag{A1}$$

and the total photon loss per unit area by the probe pulse, also known as the integrated pump–probe photon (IPPp) signal, defined by

$$N(\tau)=\frac{1}{2\pi}\int_{-\infty}^{\infty}\frac{I_{pr}(\omega,\tau)}{\hbar\omega}\,d\omega. \tag{A2}$$

Here, $I_{pr}(\omega,\tau)$ is the change in spectral intensity given by

$$I_{pr}(\omega,\tau)=\frac{z\rho_0}{3n_0}\,\mathrm{Im}[\omega\tilde{E}_2^*(\omega)P_3(\omega,\tau)], \tag{A3}$$

where z, ρ_0, and n_0 are the length, number density, and index of refraction of the sample being measured, P_3 is the third-order polarization, and $\tilde{E}_2(\omega)$ is the Fourier transformation of the probe field.

The molecule, initially in the ground state, is first excited to the intermediate excited state by the pump pulse, $E_1(t)$, and after a delay time τ is excited to the probe state by the probe pulse, $E_2(t)$. As in Sec. II, we assume that there is no overlap between the two pulses and all dephasing and relaxation is ignored. Then the third-order polarization can be explicitly written as

$$P_3(t,\tau)=\frac{1}{\hbar}\int_{-\infty}^{t}dt'E_2(t')\langle\psi_1(t'+\tau)|e^{i\hat{H}_1(t-t')/\hbar}\times\mu_2 e^{i\hat{H}_2(t-t')/\hbar}\mu_2|\psi_1(t+\tau)\rangle, \tag{A4}$$

where the pump state wave function $\psi_1(t+\tau)$ is defined as

$$\psi_1(t+\tau)=e^{i\hat{H}_1(t+\tau)/\hbar}\psi_1=e^{i\hat{H}_1t/\hbar}\psi_1(\tau), \tag{A5}$$

with $\psi_1(\tau)$ given by Eq. (11) and ψ_1 given by Eq. (12). Substitution of Eqs. (A4) and (A3) into Eq. (A2) leads to

$$\begin{aligned}N(\tau)&=\frac{z\rho_0}{n_0\hbar 6\pi}\,\mathrm{Im}\int_{-\infty}^{\infty}E_2^*(\omega)P_3(\omega,\tau)d\omega\\&=\frac{z\rho_0}{3n_0\hbar}\,\mathrm{Im}\int_{-\infty}^{\infty}E_2^*(t)P_3(t)dt\\&=\frac{z\rho_0}{3n_0\hbar^2}\,\mathrm{Re}\int_{-\infty}^{\infty}dt\int_{-\infty}^{t}dt'E_2^*(t)E_2(t')\times\langle\psi_1(t+\tau)|\mu_2 e^{i\hat{H}_2(t-t')/\hbar}\mu_2|\psi_1(t'+\tau)\rangle.\end{aligned} \tag{A6}$$

Then, by writing the real part in Eq. (A6) as the sum of the integrand and its complex conjugate and making use of the definition in Eq. (10), we arrive at the explicit expression for the IPPp signal,

$$N(\tau)=\frac{z\rho_0}{6n_0}\langle\psi_2(\tau)|\psi_2(\tau)\rangle, \tag{A7}$$

which is exactly Eq. (13), except for a constant prefactor. Finally, under the assumption that H_1 commutes with μ_2, Eq. (A1) for the IPPe signal can be reduced to

$$I(\tau)=\frac{z\rho_0}{6n_0}\langle\psi_2(\tau)|(\hat{H}_2-\hat{H}_1)|\psi_2(\tau)\rangle. \tag{A8}$$

APPENDIX B: VALIDITY OF THE FROZEN WAVE PACKET APPROXIMATION

As explained in Sec. III, the displacement of the molecular wave packet during excitation consists of a contribution from the initial velocity, Eq. (15), and a contribution from the net acceleration, Eq. (16). Here, the initial wave function of a displaced harmonic oscillator is solved to demonstrate the validity of the frozen wave packet approximation for the excitation of the ground state by a pump pulse.

To begin, the system is initially in the ground state of a displaced harmonic oscillator,

$$\psi_0=\frac{1}{(\pi\lambda^2)^{1/4}}\exp\left[-\frac{(x+d)^2}{2\lambda^2}\right], \tag{B1}$$

where λ is the Gaussian width defined as $\lambda^2=\hbar/m\omega$, with ω being the frequency of the oscillator, and d is the displacement between the ground and excited state harmonic oscillators. The quantum propagator of this system can be expressed in a closed form as

$$e^{i\hat{H}_1 t}\psi_0=\frac{1}{(\pi\lambda^2)^{1/4}}\exp\left[-\frac{(x-x_t)^2}{2\lambda^2}+\frac{ip_t(x-x_t)}{\hbar}+i\gamma_t\right], \tag{B2}$$

where

$$p_t=-\omega d\,\sin(\omega t), \tag{B3}$$

$$x_t=-d\,\cos(\omega t), \tag{B4}$$

and

$$\gamma_t=\frac{\omega^2 d^2}{4}\sin(2\omega t)+(\omega_{10}+\omega/2)t, \tag{B5}$$

with ω_{10} being the transition frequency between the excited and ground states. For simplicity, the mass m and the Planck constant $\hbar$ are not explicitly included in the above expressions.

According to Eq. (12), the initial excited state wave function is expressed as

$$\psi_1=i\mu\,\frac{1}{(\pi\lambda^2)^{1/4}}\int_{-\infty}^{\infty}e^{S(t)}E(t)dt, \tag{B6}$$

where the exponential part is

$$S(t)=-\frac{1}{2\lambda^2}\left(y-\frac{d\omega^2t^2}{2}\right)^2-iy\;d\omega^2t+i\,\frac{d^2\omega^2t}{2}+\omega_{10}t, \tag{B7}$$

with $y=x+d$ and the transition dipole moment μ being a constant. To be consistent with the quadratic form of the harmonic oscillator propagator, the electric field takes the functional form of a Gaussian,

$$E(t)=E_0e^{-i\omega_{10}t}\exp\left(\frac{-t^2}{2t_p^2}\right)+\text{c.c.}, \tag{B8}$$

where t_p is the time duration of pulse and c.c. denotes the complex conjugate. After substituting the Gaussian field of Eq. (B8) into Eq. (B6) and performing the time integration, we have

$$\begin{aligned}\psi_1&=\exp\left[-\frac{(d^2\omega^2/2-y\;d\omega^2)^2}{2(1/t_p^2-y\;d\omega^2/\lambda^2)}-\frac{y^2}{2\lambda^2}\right]\\&\approx\exp\left[-\frac{U^2}{2\Gamma^2}-\frac{y^2}{2\lambda^2}\right],\end{aligned} \tag{B9}$$

where $\Gamma=1/t_p$ and U is the potential difference. The last equality in Eq. (B9) gives rise to the classical result and is justified if

$$\frac{1}{t_p^2}\gg\frac{\omega^2yd}{\lambda}\approx\omega^2d\lambda, \tag{B10}$$

where y is in the order of the Gaussian width λ. With the introduction of $f_c=m\omega d$ as the force arising from the potential difference of the ground and excited states in the Franck–Condon region, Eq. (B10) becomes exactly the same as Eq. (16), which sets the condition for the validity of the frozen wave packet approximation: the displacement during the excitation is considerablely smaller than the characteristic width of the molecular wave packet.

APPENDIX C: FREE PARTICLE PROPAGATION OF A GAUSSIAN WAVE PACKET

To examine the free particle propagator, we assume that the wave packet at zero time takes the form of a Gaussian function

$$\psi(0)=\mathcal{N}\exp\left[-\frac{x^2}{2\lambda^2}+i\,\frac{p_cx_c}{\hbar}\right], \tag{C1}$$

where the normalization factor is

$$\mathcal{N}=\frac{1}{(\pi\lambda^2)^{1/4}}. \tag{C2}$$

Applying the free particle propagator, $e^{i\hat{K}t}$, to Eq. (C1) gives

$$\begin{aligned}\psi(t)&=e^{i\hat{K}t/\hbar}\psi(0)\\&=\mathcal{N}\sqrt{\frac{\lambda}{\lambda(t)}}\exp\left[-\frac{(x-i\lambda^2p_c/\hbar)^2}{2\lambda^2(t)}-\frac{\lambda^2p_c^2}{\hbar^2}\right]\end{aligned} \tag{C3}$$

with the time-dependent Gaussian width

$$\lambda(t)^2=\lambda^2+\frac{i\hbar t}{m\lambda}. \tag{C4}$$

After rearrangement of the exponential part, we have

$$\psi(t)=\mathcal{N}\sqrt{\frac{\lambda}{\lambda(t)}}\exp\left\{\frac{\lambda^2}{2[\lambda^4+(t/m\hbar)^2]}\left[-(x-v_ct)^2+2i\frac{x\lambda^2p_c}{\hbar}-i\lambda^2t\frac{p_c^2}{m\hbar}+i\frac{\hbar t}{m}\lambda^2x^2\right]\right\}. \tag{C5}$$

To proceed, the imaginary part in $\lambda(t)$ can be ignored if the following inequality is satisfied,

$$\frac{\hbar t}{m}\ll\lambda^2, \tag{C6}$$

where the left hand side represents the spreading of the wave packet due to quantum dispersion, which is not significant if the time is short. Under this condition, we can rewrite the wave packet as

$$\psi(t)=e^{i\hat{k}t}\psi(0)=\mathcal{N}\exp\left[-\frac{(x-v_ct)^2}{2\lambda^2}+\frac{ixp_c-(v_ct/2)}{\hbar}\right]. \tag{C7}$$

APPENDIX D: OFF-RESONANT TWO-PHOTON ABSORPTION

In contrast to the pump–probe process, two-photon absorption is a coherent multiphoton process, which means the step-wise treatment used in Sec. II is not applicable here. To gain a simple understanding of the process, we generalize the classical model in Sec. III to analyze this coherent two-photon process. To begin, we write the excited part of the wave function after the excitation as

$$\psi=\int_{-\infty}^{\infty}\int_{-\infty}^{t_2}e^{i\omega_1t_1}e^{i\omega_2t_2}E(t_2)E(t_1)\psi(t_1)dt_1\,dt_2, \tag{D1}$$

where $\hbar\omega_2=V_2-V_1$ and $\hbar\omega_1=V_1-V_0$. With the introduction of new integral variables $2s=t_2-t_1$ and $2t=t_2+t_1$ and the assumption of a Gaussian pulse as in Eq. (21) with $t_0=0$, Eq. (D1) becomes

$$\psi=\int_{-\infty}^{\infty}dt\int_{-\infty}^{0}dsE_0^2\exp\left[-\left(\frac{1}{t_p^2}+ic\right)(s^2+t^2)+i(\omega_1+\omega_2-2\omega_0)t+i(\omega_1-\omega_2)s\right]\psi(t+s). \tag{D2}$$

The intermediate state $|1\rangle$ is assumed to be off resonance, implying $d=t_p(\omega_1-\omega_2)\gg1$. Then the integration of s can be completed, resulting in

$$\psi\approx C(\Gamma)E_0^2\int\exp\left[-\left(\frac{1}{t_p^2}+ic\right)t^2+i(\omega_1+\omega_2-2\omega_0)t\right]\psi(t)dt=C(\Gamma)\int\overline{E(t)}e^{i(\omega_1+\omega_2)t}\psi(t)dt, \tag{D3}$$

where $C(\Gamma)$ is the result of the s integration, explicitly given by

$$C(\Gamma)=\frac{1}{\Gamma}\exp\left(-\frac{d^2}{4\Gamma^2}\right), \tag{D4}$$

which is a function of the bandwidth only. More importantly, as can be seen from Eq. (D3), an off-resonant two-photon process can be viewed just as a single photon process with the laser field defined by

$$\overline{E(t)}=E_0^2\exp\left[-\frac{t^2}{t_p^2}-ict^2-2\omega_0t\right], \tag{D5}$$

which, in comparison to the original form of the Gaussian pulse in Eq. (21), has double the carrier frequency, double the chirp rate, and the square of the field.

APPENDIX E: OPTIMIZATION OF A SEQUENTIAL MULTIPULSE PROCESS

We begin by considering a sequential multiphoton process consisting of N nonoverlapping laser pulses given as

$$\epsilon(t)=\sum_{n=1}^{N}[E_n(t)e^{-i\omega_nt}+E_n^*(t)e^{i\omega_nt}], \tag{E1}$$

where the electric fields $E_n(t)$ are localized in time with the subscript n denoting the sequence of time. Here, the light pulses are designed in such a way that ω_n corresponds to an electronic transition frequency from state $|l_{n-1}\rangle$ to state $|l_n\rangle$ and so that, under the rotating wave approximation the molecule, starts from the ground state $|0\rangle$, goes through intermediate excited states $|l_n\rangle$, and reaches the final state $|l_N\rangle$. As a result of the excitation, the molecule on the final electronic state $|l_N\rangle$ can be described by a density matrix given by

$$\hat{\rho}_N(t_f)=G_N(t_f-T_N)\cdots G_1(t_2-t_1):G_0(t_1-t_i)\times\hat{\rho}_0G_0^+(t_1-t_i):G_1^+(t_2-t_1)\cdots G_N^+(t_f-t_N), \tag{E2}$$

where $G_n(t_{n+1}-t_n)$ is the propagator on the $|l_n\rangle$ electronic potential surface

$$G_n(t_{n+1}-t_n)=\exp[-i\hat{H}_{l_n}(t_{n+1}-t_n)/\hbar], \tag{E3}$$

with $\hat{H}_{l_n}$ being the corresponding Hamiltonian. Here, the colon represents an electronic excitation defined by

$$G_n(t_{n+1}-t_n):G_{n-1}(t_n-t_{n-1})=\frac{1}{\hbar}\int_{t_l}^{t_f}G_n(t_{n+1}-t_n)\mu_nG_{n-1}(t_n-t_{n-1})E(t_n), \tag{E4}$$

with μ_n being the transition dipole moment between states $|l_{n-1}\rangle$ and $|l_n\rangle$. The notation introduced above simplifies the analysis for the optimization of the multiphoton process.

In general, the target of quantum control can be specified as an operator $\hat{A}$ and the degree of control is measured by the expectation value of this target operator at time t_f, or explicitly,

$$A(t_f)=\mathrm{Tr}[\hat{A}\hat{\rho}(t_f)], \tag{E5}$$

where the target is defined on the final electronic state manifold. In the weak response regime, the analysis is simplified by linearizing the Liouville operator in terms of field. Assume that the initial density matrix is defined on the ground state, $\hat{\rho}_0$, and the target operator is defined on the final excited state, $\hat{A}=\hat{A}_{l_N}|l_N\rangle\langle l_N|$; then the leading term of the expectation value of the target is

$$A(t_f)=\int_{t_i}^{t_f} dt \int_{t_l}^{t_f} dt' E_n^*(t) M_n(t,t') E_n(t'), \tag{E6}$$

where the material response function matrix M is defined by

$$M_n(t,t')=\frac{1}{\hbar^2}\,\mathrm{Tr}[A_n(t_n,t_n')\rho_n(t_n',t_n)]. \tag{E7}$$

Here, the time-dependent density operator and target operator are defined as

$$\hat{A}_n=G_n^+ : G_{n+1}^+ \cdots G_{l_N}^+ \hat{A}_N G_N \cdots G_{n+1} : G_n \tag{E8}$$

and

$$\hat{\rho}_n=G_{n-1}\cdots G_1 : G_0\hat{\rho}_0 G_0^+ : G_1^+ \cdots G_{n-1}^+ . \tag{E9}$$

The goal of control is to find an external field $E(t)$ which maximizes the realization of the target under certain constraints. To this end, we construct a functional as

$$J(t_f)=A(t_f)-\eta\int_{t_0}^{t_f}|E(t)|^2\,dt, \tag{E10}$$

where the Lagrange multiplier η is introduced to lift the constraint on the total radiation energy.[26] Rigorously, the optimization of the laser field can be achieved by a variational differentiation of the functional $J(t_f)$ with respect to the field, $\delta J(t_f)/\delta E^*(t)=0$. In the weak response regime, an application of the variational procedure results in a linear field equation

$$\int_{t_i}^{t_f} M_n(t,t')E_n(t')dt'=\eta_n E_n(t), \tag{E11}$$

which can be solved as a conventional eigenvalue problem. The eigenequation holds for every individual field, i.e., $n=1,...,N$, and the optimization is achieved by solving the N eigenequations simultaneously.

Recently Cao and Yan have formulated two-photon optimal control as an eigenvalue problem such that the two optimal fields satisfy a rigorous time-reversal relationship.[32] This result is significant for optimizing the pump–dump control scheme[9] as a method to efficiently transfer population to a highly excited vibrational eigenstate.

[1] A. H. Zewail, in *Femtosecond Chemistry*, edited by J. Manz and L. Wöste (Springer-Verlag, Weinheim, 1995), p. 15.
[2] R. Bersohn and A. H. Zewail, Ber. Bunsenges. Phys. Chem. **92**, 373 (1988).
[3] R. E. Walkup, J. A. Misewich, J. H. Glownia, and P. P. Sorokin, Phys. Rev. Lett. **65**, 2366 (1990).
[4] B. Fain, S. H. Lin, and N. Hamer, J. Chem. Phys. **91**, 4485 (1989).
[5] W. T. Pollard, S.-Y. Lee, and R. A. Mathies, J. Chem. Phys. **92**, 4012 (1990).
[6] Y. J. Yan, L. E. Fried, and S. Mukamel, J. Phys. Chem. **93**, 8149 (1989).
[7] Y. J. Yan and S. Mukamel, Phys. Rev. A **41**, 6485 (1990).
[8] S. Y. Lee, in *Femtosecond Chemistry*, edited by J. Manz and L. Wöste (Springer-Verlag, Weinheim, 1995), p. 273.
[9] D. J. Tannor and S. A. Rice, J. Chem. Phys. **83**, 5013 (1985).
[10] J. K. Krause, R. M. Whitnell, K. R. Wilson, and Y. J. Yan, in *Femtosecond Chemistry*, edited by J. Manz and L. Wöste (Springer-Verlag, Weinheim, 1995), page 743.
[11] Y. J. Yan, J. Chem. Phys. **100**, 1094 (1994).
[12] J. Che, J. L. Krause, M. Messina, K. R. Wilson, and Y. J. Yan, J. Phys. Chem. **99**, 14 949 (1995).
[13] M. Sterling, R. Zadoyan, and V. A. Apkarian, J. Chem. Phys. **104**, 6497 (1996).
[14] R. M. Bowman, M. Dantus, and A. H. Zewail, Chem. Phys. Lett. **161**, 297 (1989).
[15] R. B. Bernstein and A. H. Zewail, Chem. Phys. Lett. **170**, 321 (1990).
[16] J. H. Glownia, J. A. Misewich, and P. P. Sorokin, J. Chem. Phys. **92**, 3335 (1990).
[17] Y. J. Yan and S. Mukamel, J. Chem. Phys. **88**, 5735 (1988).
[18] J. A. Cina and T. J. Smith, J. Chem. Phys. **98**, 9211 (1993).
[19] T. J. Smith and J. A. Cina, J. Chem. Phys. **104**, 1272 (1996).
[20] U. Banin, A. Bartana, S. Ruhman, and R. Kosloff, J. Chem. Phys. **101**, 8571 (1994).
[21] J. Cao and K. R. Wilson, J. Chem. Phys. (submitted).
[22] D. J. Tannor, R. Kosloff, and S. A. Rice, J. Chem. Phys. **85**, 5805 (1986).
[23] R. Kosloff, S. A. Rice, P. Gaspard, S. Tersigni, and D. J. Tannor, Chem. Phys. **139**, 201 (1989).
[24] R. S. Judson and H. Rabitz, Phys. Rev. Lett. **68**, 1500 (1992).
[25] R. Demiralp and H. Rabitz, Phys. Rev. A **47**, 809 (1993).
[26] Y. J. Yan, R. E. Gillilan, R. M. Whitnell, K. R. Wilson, and S. Mukamel, J. Phys. Chem. **97**, 2320 (1993).
[27] B. Kohler, V. V. Yakovlev, J. Che, J. L. Krause, M. Messina, K. R. Wilson, N. Schwentner, R. M. Whitnell, and Y. J. Yan, Phys. Rev. Lett. **74**, 3360 (1995).
[28] B. Kohler, J. Krause, F. Raksi, K. R. Wilson, R. M. Whitnell, V. V. Yakovlev, and Y. J. Yan, Acct. Chem. Res. **28**, 133 (1995).
[29] S. A. Rice, Science **258**, 412 (1992).
[30] E. J. Heller, Acc. Chem. Res. **14**, 368 (1981).
[31] S. Y. Lee and E. J. Heller, J. Chem. Phys. **71**, 4777 (1979).
[32] J. Cao and Y. J. Yan, J. Chem. Phys. (to be submitted).